Motion Parameter Estimation of Doppler-Ambiguous Moving Targets in SAR-GMTI

Martina Gabele
German Aerospace Center (DLR) – Wessling
Satellite SAR Systems Section
Muenchner Str. 20, 82234 Wessling, Germany
E-mail: Martina.Gabele@dlr.de

Ishuwa Sikaneta
Defence R&D Canada – Ottawa
Radar Systems Section
3701 Carling Ave., Ottawa, ON, Canada, K1A 0Z4
E-mail: ishuwa.sikaneta@drdc-rddc.gc.ca

***Abstract*— Classical SAR algorithms for focusing the signal energy of stationary targets are wavenumber domain algorithm and chirp scaling algorithm. In the paper these algorithms are adapted to focusing of moving targets. Focusing of moving targets appearing in various PRF bands is addressed as well as focusing of moving targets distributed over two neighboring PRF bands. Finally, it is shown that focusing moving targets in range and azimuth not only improves SCR, but can also help in resolving Doppler ambiguities in target motion parameter estimation.**

I. Introduction

For moving target motion parameter estimation with SAR processing it is desirable to maximize the compressed moving target peak power. In the most basic SAR compression algorithm, only the signal measurements in each single range gate are summed. This algorithm suffers from the fact that as the range to the target changes, either due to the geometry or due to target motion, the target energy manifests in different range gates. More sophisticated techniques such as the chirp scaling, [1], [2], and the wavenumber domain processor, [3]–[5], track and sum the target energy as it wanders through the range cells, but these algorithms are designed to compensate for the range cell migration of stationary targets.

Two algorithms developed specifically to SAR compress moving targets include the keystone mapping technique of [6] and the post processing technique of [7]. The keystone mapping procedure corrects improper compression of the target energy by estimating and correcting inaccurate Doppler rates and higher order Doppler rate non-linearities. This is accomplished without prior knowledge about the moving target in the range-frequency slow-time domain, and can be applied even when the target has not been adequately sampled by the PRF. The main drawback of this model-free approach is that no estimates of the target state vector are provided. In the post-processing technique of [7], the processed SAR image is further processed to better compress the moving targets. This approach is model based and can provide an estimate of the relative velocity $v_{rel}^2 = (1 - v_x/v_p)^2 + (v_y/v_p)^2$, where v_p denotes the platform velocity, v_x the target along-track velocity, and v_y the target across-track velocity. However, it does not estimate v_x, v_y separately, and it has not been extended to the case where the target has not been adequately sampled by the PRF.

We aim to extend the wavenumber domain algorithm and the extended chirp scaling algrithm so that the energy from moving targets occupying arbitrary Doppler frequency intervals is tracked through range bins and summed to form the maximum possible peak response. Finally, it is shown how the Doppler ambiguities that result from an inadequate PRF can be resolved by use of the range walk information.

II. Adaption of SAR algorithms to GMTI

In this section the wavenumber domain algorithm and the chirp scaling algorithm are adapted to focusing of moving targets with velocities v_x, v_y, where it is assumed that the whole moving target signal is Nyquist sampled.

A. Wavenumber domain algorithm for GMTI

The subsection modifies the wavecone, [3], [8] to accommodate constant velocity target motion in the along and across-track directions. The approach starts with the exploding source method of [3], [9]. Consider the range equation $R(t)$ modified to include a constant velocity target

$$R(t) = \sqrt{(v_p t - v_x t)^2 + (y + v_y t)^2}, \tag{1}$$

The x coordinate of the receiver is given by $x = v_p t - x_0$, the range position at slant range is y, and we can assume without loss of generality that $x_0 = 0$ so that $t = x/v_p$. The range equation can be presented as

$$\begin{aligned} R(x,y) &= \sqrt{\left(x - x\frac{v_x}{v_p}\right)^2 + \left(y + x\frac{v_y}{v_p}\right)^2} \\ &= \sqrt{\left(\alpha x + \frac{\beta}{\alpha} y\right)^2 + y^2\left(\frac{\alpha^2 - \beta^2}{\alpha^2}\right)}, \end{aligned} \tag{2}$$

$$\alpha^2 = \left(1 - \frac{v_x}{v_p}\right)^2 + \left(\frac{v_y}{v_p}\right)^2, \tag{3}$$

$$\beta^2 = \left(\frac{v_y}{v_p}\right)^2. \tag{4}$$

Now, in similar fashion to the development in [10], suppose that there exists a space defined by

$$\vec{u} = \begin{bmatrix} \alpha & \frac{\beta}{\alpha} \\ 0 & \sqrt{\frac{\alpha^2 - \beta^2}{\alpha^2}} \end{bmatrix} \vec{x} = \boldsymbol{A}\vec{x}, \quad \vec{x} = \begin{bmatrix} x \\ y \end{bmatrix}. \tag{5}$$

The change of coordinates yields the following equation for an exploding source

$$u^2 + v^2 = \frac{c^2}{4}t^2, \tag{6}$$

Consider the 2D Fourier transform

$$F_x(\vec{k}) = \int f(\vec{x})e^{-j\vec{k}^\dagger\vec{x}}\mathrm{d}\vec{x}, \tag{7}$$

where the function $f(\vec{x})$ describes the terrain in the $\vec{x}$ coordinate system. Let it be that in the $\vec{u}$ coordinate system, the same terrain is described by the function $g(\vec{u})$. One then has that

$$F_u(\vec{k}) = \int g(\vec{u})e^{-j\vec{k}^\dagger\vec{u}}\mathrm{d}\vec{u}. \tag{8}$$

With $\vec{u} = \boldsymbol{A}\vec{x}$, we have that $\mathrm{d}\vec{u} = |A|\mathrm{d}\vec{x} = \det\boldsymbol{A}\mathrm{d}\vec{x}$; thus $F_u(\vec{k}) = |A|F_x(\boldsymbol{A}^\dagger\vec{k})$. We know from [3], [8] how to migrate $S(u, v = 0, t)$ to $S(u, v, t = 0)$ using a Stolt interpolation given by

$$S_u(k_u, k_v, t = 0) = \frac{c}{2}\frac{k_v}{|\vec{k}|}S_u\left(k_u, v = 0, \omega = \frac{c}{2}\mathrm{sgn}(k_v)|\vec{k}|\right), \tag{9}$$

therefore, $S_x(\vec{k}, t = 0) = |A|^{-1}S_u((\boldsymbol{A}^\dagger)^{-1}\vec{k}, t = 0)$. A short computation shows that

$$(\boldsymbol{A}^\dagger)^{-1} = \begin{bmatrix} \alpha^{-1} & 0 \\ -\frac{\beta}{\alpha^2}\sqrt{\frac{\alpha^2}{\alpha^2-\beta^2}} & \sqrt{\frac{\alpha^2}{\alpha^2-\beta^2}} \end{bmatrix}, \tag{10}$$

Thus

$$\vec{k} \to (\boldsymbol{A}^\dagger)^{-1}\vec{k} = \begin{bmatrix} \frac{k_x}{\alpha} \\ \sqrt{\frac{\alpha^2}{\alpha^2-\beta^2}}\left(k_y - \frac{\beta}{\alpha}\frac{k_x}{\alpha}\right) \end{bmatrix}. \tag{11}$$

With $S_u(k_u, v = 0, \omega) = \alpha S_x(\alpha k_u, y = 0, \omega)$,

$$S_x(\vec{k}, t = 0) = \frac{\alpha^2 c}{2}\frac{k_y - \frac{\beta}{\alpha}\frac{k_x}{\alpha}}{\sqrt{\left(\frac{k_x}{\alpha}\right)^2 + \frac{\alpha^2}{\alpha^2-\beta^2}\left(k_y - \frac{\beta}{\alpha}\frac{k_x}{\alpha}\right)^2}} \cdot S_x\left(k_x, y = 0, \omega\right), \tag{12}$$

where the frequencies ω at which to interpolate are:

$$\omega = \sqrt{\left(\frac{k_x}{\alpha}\right)^2 + \frac{\alpha^2}{\alpha^2-\beta^2}\left(k_y - \frac{\beta}{\alpha}\frac{k_x}{\alpha}\right)^2} \cdot\frac{c}{2}\mathrm{sgn}\left(k_y - \frac{\beta}{\alpha}\frac{k_x}{\alpha}\right). \tag{13}$$

The wavenumbers k_x and k_y are vectors with length equal to the number of azimuth samples for k_x respectively the number of range samples for k_y:

$$k_x = \frac{2\pi f}{v_p}, \qquad f = \left[-\frac{PRF}{2}, \frac{PRF}{2}\right], \tag{14}$$

$$k_y = \frac{4\pi}{c}\left(f_y + f_c\right), \quad f_y = \left[-\frac{f_s}{2}, \frac{f_s}{2}\right], \tag{15}$$

where f is Doppler frequency, f_y is range frequency, PRF is the pulse repetition frequency, v_p is the platform velocity, c the speed of light, f_s the fast time (range) sampling frequency, and f_c the radar carrier frequency.

B. Extended chirp scaling algorithm for GMTI

A second order Taylor expansion of (1) evidences that the range history of a moving target is equivalent to the quadratic range history of a stationary target at shifted azimuth time $\Delta t = -yv_y/v_{rel}^2$ and minimum slant range shifted by $\Delta y = -v_y^2 y/(2v_{rel}^2)$ with $v_{rel} = \sqrt{(v_p - v_x)^2 + v_y^2}$:

$$R(t) = \frac{v_{rel}^2}{2y}\left(t + \frac{yv_y}{v_{rel}^2}\right)^2 + y - \frac{v_y^2 y}{2v_{rel}^2}. \tag{16}$$

The moving target raw data signal is a non-centered cutout of the quadratic range history with slightly modified parameters. In the following, this knowledge is incorporated into the extended chirp scaling algorithm [2].

First, the chirp scaling algorithm performs range scaling in y-f domain in order to equalize the range cell migration at each range to the range cell migration of a target with velocities v_x, v_y at reference range y_r:

$$H_1(f, y) = \exp\left\{-j\frac{2\pi}{c}k(f)a(f)\left[y - R(f)\right]^2\right\} \cdot \exp\left\{j\frac{2\pi}{c}k(f_t)a(f_t)\left[y - R(f_t)\right]^2\right\}. \tag{17}$$

The Doppler frequency vector f is defined in (14), the moving target Doppler frequency is $f_t = -2v_y/\lambda$, and

$$k(f) = \left(\frac{1}{k_r} - \frac{2\lambda y_r\left(\beta^2(f) - 1\right)}{c^2\beta^3(f)}\right)^{-1}, \tag{18}$$

$$a(f) = \frac{1}{\beta(f)} - 1, \tag{19}$$

$$R(f) = \frac{y_r}{\beta(f)}, \tag{20}$$

$$\beta(f) = \sqrt{1 - \left(\frac{f\lambda}{2v_{rel}}\right)^2}. \tag{21}$$

Furthermore, k_r is the range chirp modulation rate, and λ the carrier wavelength. Range compression and range cell migration are performed in f_y-f domain. In order to focus the target at the range position of broadside time the following processing is required:

$$H_2(f, f_y) = \exp\left\{-j\frac{\pi f_y^2}{k(f)(1 + a(f))}\right\} \cdot \exp\left\{j\frac{4\pi y_r f_y}{c}\left[a(f) - a(f_t)\right]\right\}. \tag{22}$$

The correction of the residual phase term due to the chirp and range scaling operation becomes:

$$H_3(f, y) = \exp\left\{j\frac{4\pi\left(y - y_r\right)^2 k(f)a(f)\left(1 + a(f)\right)}{c^2}\right\} \cdot \exp\left\{-j\frac{4\pi\left(y - y_r\right)^2 k(f_t)a(f_t)\left(1 + a(f_t)\right)}{c^2}\right\}. \tag{23}$$

In order to focus the target at its correct azimuth position a convolution with the following azimuth compression function is required:

$$h_4(x,y) = \exp\left[j\frac{2\pi x^2}{\lambda y}\right] \cdot \exp\left[-j\frac{4\pi x v_y}{\lambda v_{rel}}\right], \qquad (24)$$

where x is again the azimuth position of the platform.

III. Doppler subsampled target signals

For extending the target velocity interval of interest to signals that are azimuth subsampled we analyze fast moving target signals with respect to range cell migration, azimuth position, and along-track interferometric phase. In the following, moving target signals with velocities that are not Nyquist sampled, are called fast moving targets. Slow moving targets we call target signals that are Nyquist sampled.

A. Range cell migration

If the target energy is in PRF bands other than the Nyquist band, the signal is backfolded in Doppler frequency domain. Consequently, the signal of a fast moving target is the same as the signal of its corresponding slow moving target with respect to the azimuth component. However, the signals differ in their range component. The range cell migration of slow and fast moving targets versus Doppler frequency as it appears in the Nyquist band is sketched in figure 1. It is obvious, that the range cell migration is Doppler unambiguous.

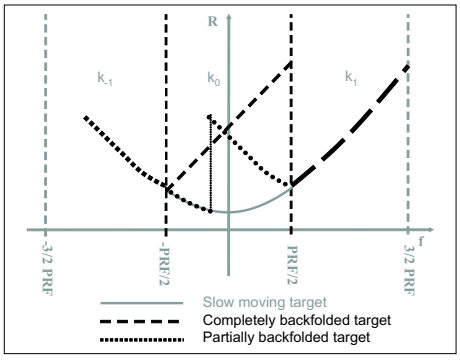

Fig. 1. Range migration R versus Doppler frequency f for slow and fast moving targets.

B. Along-track interferometric phase

In order to determine the along-track interferometric (ATI) phase coregistration of the data is required. In the coregistration procedure the data from two channels which were recorded at the same sampling time, but from different along-track positions, are interpolated such that the sampling positions of both channels are at the same positions, but at different sampling times. The time shift corresponds to a multiplication with a phase ramp in Doppler frequency domain. For a spatial separation d of the two receivers the interferometric phase ramp $\phi(f, v_y)$ is

$$\phi(f, v_y) = \frac{\pi d}{v_{rel}} f + \frac{2\pi d}{\lambda}\frac{v_y}{v_a}. \qquad (25)$$

For coregistration the inverse clutter phase ramp $-\phi(f,0)$ has to be applied. If the moving target signal is backfolded in Doppler frequency domain ($k_n \neq 0$), the inverse clutter interferometric phase ramp applies a phase correction to the target signal that stems from a Doppler frequency which is $k_n PRF$, $k_n = \pm 1, \pm 2, ...$ higher respectively lower than the actual frequency. The ATI phase $\phi(v_y)$ is:

$$\phi(v_y) = \frac{2\pi d}{\lambda}\frac{v_y}{v_a} + \frac{\pi d}{v_a} k_n PRF, \qquad (26)$$

where $k_n \leq 0$ if $v_y > 0$ and vice versa (e.g. k_1 characterizes the next higher PRF band, and k_{-1} the next lower PRF band). The quantity of the phase jump $\Delta\phi = \phi(k_n) - \phi(k_{n-1})$ depends only on the system parameters, but not on v_y. For completely backfolded target signals (k_n is the same for the whole signal) the phase jump has to be taken into account in order to determine which target velocities v_y have to be considered for a certain ATI phase. For partially backfolded target signals (k_n is different for different frequency intervals of the signal) the phase jump has to be compensated in the SAR compression filter, otherwise the signals do not sum up coherently, the magnitude of the SAR impulse response degrades and the ATI phase information is destroyed.

C. Azimuth position

The Doppler frequency history $f(t)$ of a moving target is

$$f(t) = -\frac{2v_{rel}^2}{\lambda y} t - \frac{2v_y}{\lambda} - k_n PRF. \qquad (27)$$

Since the azimuth position in a stationary world SAR filter is given by the zero crossing $f(t) = 0$, the azimuth position after SAR compression $\tilde{x}_0$ is

$$\tilde{x}_0 = -\frac{\lambda y}{2v_a}\left(\frac{2v_y}{\lambda} + k_n PRF\right). \qquad (28)$$

This means not only the ATI phase, but also the azimuth position is backfolded in case of Doppler backfolding. In figure 2 on the left the azimuth position, on the right the ATI phase versus across-track velocity is shown. In each case the higher signal energy part is used in case of partial backfolding.

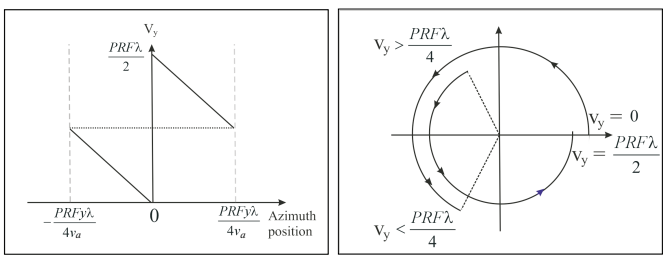

Fig. 2. Left: Azimuth position versus across-track velocity for stationary world matched filter, right: ATI phase as a function of across-track velocity.

D. Extension of SAR algorithms

If Doppler ambiguous target signals shall be focused, the SAR processing has to be extended to properly range-compress Doppler backfolded target signals, because range cell migration is Doppler unambiguous. The adaption is accomplished by choosing the Doppler frequency interval correspondingly:

$$f = \left[-\frac{PRF}{2} + f_t, \frac{PRF}{2} + f_t \right], \tag{29}$$

If the target energy is spread over two neighboring PRF bands the Doppler frequency vector has to be shifted circularly such that it fits the order of the moving target Doppler frequency samples after backfolding.

IV. Motion parameter estimation of Doppler ambiguous moving target signals

A. Along-track velocity estimation

The moving target along-track velocity v_x impacts on the azimuth focusing of the target signal. Hence, assuming constant v_x, v_y the along-track velocity can be concluded from the azimuth focusing of the target signal.

B. Across-track velocity estimation

Across-track velocity estimation by use of the ATI phase is Doppler ambiguous in intervals of $\Delta v_y = PRF\lambda/2$. Since range cell migration is Doppler unambiguous, the magnitude of the target impulse response focusing in azimuth and range to the potential target velocities with the same ATI phase can help in resolving these ambiguities.

C. Azimuth position estimation

Comparing the azimuth displacement jump concluded from the ATI phase (26) and the actual azimuth position jump (28) of Doppler backfolded signals yields the same result. This means that the position estimation is not Doppler ambiguous and is estimated correctly as long as there are only Doppler ambiguities, but no angle ambiguities. However, a moving target distributed over two neighboring PRF bands may look like two moving targets with different across-track velocities shifted away from the same azimuth position. The two signals can be identified as potentially two parts of the same target due to a characteristic separation in azimuth position and ATI phase.

A strategy for target motion parameter estimation is the following: First, the azimuth compression is optimized by varying v_{rel} without performing range cell migration correction. From the in azimuth direction well-focused signal the possible target across-track velocities v_y can be concluded e.g. from the ATI phase, and v_x can be concluded from v_{rel}. Feeding v_x and v_y into a SAR processor that adapts to moving target velocities, focuses the target at the correct azimuth position. Next, the ambiguities in v_y which may result from Doppler backfolding of the target signal, can be resolved by feeding v_x and v_y into a processor, which performs SAR compression with range cell migration correction adapted to v_x, v_y (II-A, II-B). The v_y which yields the highest SAR impulse response due to proper range cell migration correction, is chosen to be the right v_y.

V. Simulations

In figure 3 the focusing of two fast moving, partially backfolded target signals by adaption of the wavenumber domain respectively extended chirp scaling algorithm to the target motion parameters are shown. The system parameters chosen are from the Canadian experimental airborne two-channel radar Convair 580. With both algorithms the target impulse response appears at the correct azimuth and range position. The lessened focusing of the wavenumber domain algorithm in case of the very fast moving target is probably due to the interpolation step required in this processor.

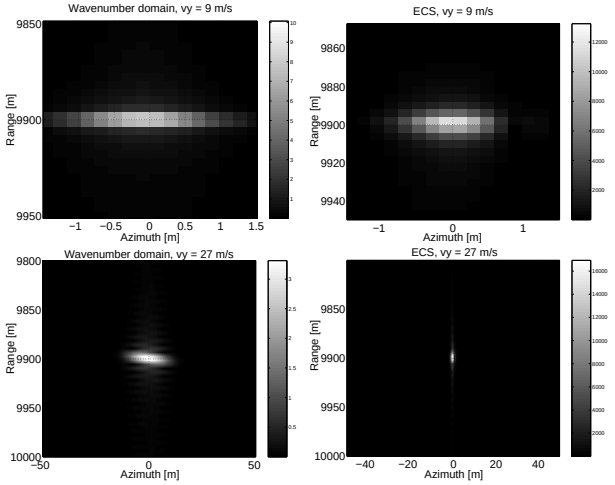

Fig. 3. Top: focusing partially backfolded fast moving target signal ($v_y = 9m/s$), bottom: focusing partially backfolded very fast moving target signal ($v_y = 27m/s$), left: wavenumber domain algorithm, right: extended chirp scaling algorithm. ($x_0 = 0m$, $y = 9900m$, Convair 580 system parameters.)

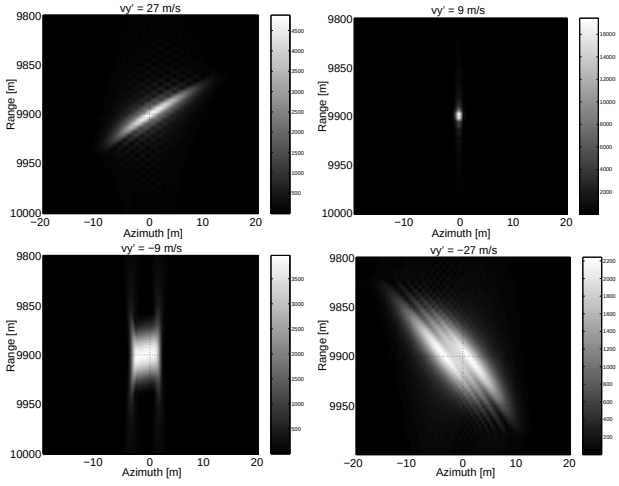

Fig. 4. Target impulse response on focusing with the chirp scaling algorithm and various matched filter velocities v_y'. (True target velocity $v_y = 9m/s$, Convair 580 system parameters.)

In figure 4 the difference in magnitude of the impulse response for using the chirp scaling processor adapted to various target velocities which yield the same ATI phase is shown. The difference in magnitude is a factor of 3 to 4 for a separation of one PRF band from the true target velocity, and a factor of about 8 for a separation of two PRF bands.

VI. Experimental data results

In this section the strategy for Doppler ambiguous target motion parameter estimation described in section IV is demonstrated with a real data example from the Canadian experimental airborne radar system Convair 580. The ATI phase of the target raw data signal is shown in figure 5 on the left. It can be seen, that the ATI phase is different for the part of the signal in the upper right corner of the image. This means that this is a partially backfolded target signal. Varying v_{rel} in order to optimize azimuth focusing yields $v_{rel} = 100m/s$. (This is a realistic value because for real data the assumption of constant target velocities is often not valid.) The ATI phase indicates $v_y = 24.9m/s$, $v_y = 6.9m/s$, $v_y = -11.1m/s$ or $v_y = -29.1m/s$.

Next, the data are fed to a SAR processor which performs range cell migration correction adapted to moving target velocities. In figure 6 the DPCA images after SAR focusing the target signal with the chirp scaling algorithm using two possible target across-track velocities are shown. As could be seen already in the simulation results in figure 4 there is about a factor of 3 to 4 between the magnitude of impulse responses on a target velocity one PRF band apart, and in this case a factor of about 6 for target velocities two PRF bands apart from the true target velocity v_y. This indicates that $v_y = -11.1m/s$ is the true target across-track velocity. The ATI polar plot of the target signal focused with the chirp scaling algorithm adapted to the target velocities and phase jump corrected is shown in figure 5 on the right. The ATI phase information is well preserved.

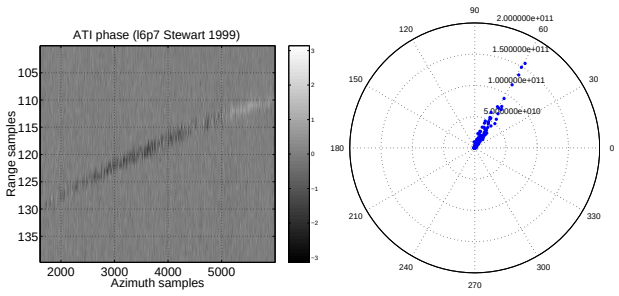

Fig. 5. Left: ATI raw data image (l6p7 Stewart 1999, Convair 580), right: ATI polar plot of the processed image (chirp scaling algorithm adapted to the target signal($v_{rel} = 100m/s$, $v_y = -11.1m/s$ and phase jump correction)

VII. Summary

In this paper we derived the wavenumber domain and the extended chirp scaling algorithm for SAR focusing moving target signals with constant velocities v_x, v_y. The processing is then extended to Doppler subsampled target signals. Finally, it is shown, that the range cell migration information, which is Doppler unambiguous, can be used for resolving Doppler ambiguities in target motion parameter estimation.

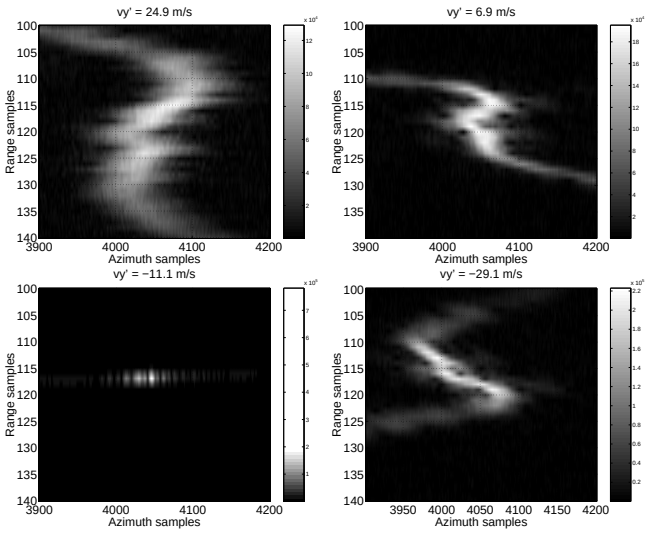

Fig. 6. Target impulse response on focusing with the chirp scaling algorithm and various matched filter velocities v_y'.

VIII. Acknowledgements

The authors would like to thank Dr. Chuck Livingstone and DRDC for providing the data used in the analysis.

References

[1] Runge, H. and Bamler, R., *A Novel High Precision SAR Focussing Algorithm Based On Chirp Scaling*, IGARSS, Houston (Texas), May 1992

[2] Moreira, A., Mittermayer, J. and Scheiber, R., *Extended chirp scaling algorithm for air- and spaceborne SAR data processing in stripmap and ScanSAR imaging modes*, IEEE Transactions on Geoscience and Remote Sensing, vol. 34, no. 5, pages 1123-1136, September 1996

[3] Caffario, C., Prati, C. and Rocca, F., *SAR data focusing using seismic migration techniques*, IEEE Transactions on Aerospace and Electronic Systems, vol. 27, no. 2, pages 194-207, March 1991

[4] Cobb, M.C. and McClellan, J.H., *Omega-k quadtree UWB SAR focusing*, Radar Conference, IEEE Proceedings, May 2001

[5] Cumming, I.G., Neo, Y.L. and Wong, F.H., *Interpretations of the omega-K algorithm and comparisons with other algorithms*, IGARSS, Toulouse (France), July 2003

[6] Perry, R.P., DiPietro, R.C. and Fante, R.L., *SAR imaging of moving targets*, IEEE Transactions on Aerospace and Electronic Systems, vol. 35, no. 1, pages 188-200, January 1999

[7] Jen King Jao, *Theory of synthetic aperture radar imaging of a moving target*, IEEE Transactions on Geoscience and Remote Sensing, vol. 39, no. 9, pages 1984-1992, September 2001

[8] Bamler, R., *A comparison of range-Doppler and wavenumber domain SAR focusing algorithms*, IEEE Transactions on Geoscience and Remote Sensing, vol. 30, no. 4, pages 706-713, July 1992

[9] Claerbout, J. F., *Imaging the Earth's Interior*, Blackwell Science Inc., 1985

[10] Soumekh, M., *Synthetic Aperture Radar Signal Processing With MATLAB Algorithms*, Wiley and Sons, New York, 1999

[11] Gierull, C. H., *Moving Target Detection with Along-Track SAR Interferometry*, Defence Research and Development Canada Technical Report, January 2002